



On-Surface Chemistry on Low-Reactive Surfaces

Elie Geagea, Frank Palmينو, Frédéric Cherioux

► To cite this version:

Elie Geagea, Frank Palmينو, Frédéric Cherioux. On-Surface Chemistry on Low-Reactive Surfaces. Chemistry, 2022, 4, pp.796 - 810. <hal-03818555>

HAL Id: hal-03818555

<https://hal.science/hal-03818555v1>

Submitted on 18 Oct 2022

HAL is a multi-disciplinary open access archive for the deposit and dissemination of scientific research documents, whether they are published or not. The documents may come from teaching and research institutions in France or abroad, or from public or private research centers.

L'archive ouverte pluridisciplinaire **HAL**, est destinée au dépôt et à la diffusion de documents scientifiques de niveau recherche, publiés ou non, émanant des établissements d'enseignement et de recherche français ou étrangers, des laboratoires publics ou privés.



HAL Authorization

On-surface chemistry on low-reactive surfaces

Elie GEAGEA ¹, Frank PALMINO ¹ and Frédéric CHERIOUX ^{1,*}

¹ Université de Franche-Comté, FEMTO-ST, CNRS, UFC. 15B avenue des montboucons, F-25030 BESANCON cedex, France.

* Correspondence: frederic.cherieux@femto-st.fr

Abstract: zero-dimensional (0D), mono-dimensional (1D), or two-dimensional (2D) nanostructures with well-defined properties fabricated directly on surfaces are of growing interest. The fabrication of covalently bound nanostructures on non-metallic surfaces is very promising in terms of applications, but the lack of surface-assistance during their synthesis is still a challenge to achieve the fabrication of large-scale and defect-free nanostructures. We discuss the state-of-the-art approaches recently developed in order to provide covalently bounded nanoarchitectures on passivated metallic surfaces, semiconductors and insulators.

Keywords: Surface science; STM; AFM; Synthesis; On-surface chemistry.

1. Introduction

On-surface chemistry, i. e. the bottom-up construction of covalent bonds between molecular building blocks adsorbed on a surface, has been greatly developed during the last two decades. [1–18] Indeed, the use of nanomaterials spans a wide range of sectors, like healthcare, electronics, photonics, chemistry, energy, etc. Nanoengineered materials are designed to have increased structural strength, chemical sensitivity, conductivity, and improved overall properties, with great potential in materials innovation. In this perspective, the reliable elaboration of components based on nanostructured materials, with atomically precise control over their structure and/or functionalities is still challenging. The development of on-surface chemistry was also strongly improved thanks to the development of scanning probe microscopies, scanning tunneling microscopy -STM- and atomic force microscopy -AFM-, under ultra-high vacuum (UHV) [19, 20]. Most of results have been obtained on low index metallic surfaces such as Au(111), Ag(111) and Cu(111). This is due to the overlapping of molecular orbitals with the electronic structure of the underlying surface which promotes surface-assisted formation of C-C bonds in terms of oxidative addition/reductive elimination sequences or in terms of surface-assisted stabilization of radicals [5]. Unfortunately, the strong interaction of the molecules with the metallic surface, for example, due to hybridization of molecular states with electronic bands from the metallic substrate, often alters the electronic properties of the molecules and, moreover, can even turn off their functionality. The cases of photonic or electronic properties are the most impacted by the overlapping between molecules and surface due to the competition with the quenching of radiative decay and the transport through the surface, respectively [21]. To circumvent these disadvantages, three main strategies are currently investigated: (i) lateral manipulation with a local probe [22], (ii) intercalation of chemical species of the upper metal layers and (iii) the use of non-metallic surfaces. Basically, the two first ways consist in increasing the spacing between nanostructures and metallic surfaces to decouple the adlayer from the metal surfaces. The third way has been more recently developed [23–25]. It requires to tackle some important scientific challenges: How to compensate for the lack of surface-assistance on metal substrates to cleave and create covalent bonds? How to compensate the desorption or diffusion of all involved

Citation: Lastname, F.; Lastname, F.; Lastname, F. Title. *Chemistry* **2022**, *4*, Firstpage–Lastpage.
<https://doi.org/10.3390/xxxxx>

Academic Editor: Firstname Lastname

Received: date

Accepted: date

Published: date

Publisher's Note: MDPI stays neutral with regard to jurisdictional claims in published maps and institutional affiliations.



Copyright: © 2022 by the authors. Submitted for possible open access publication under the terms and conditions of the Creative Commons Attribution (CC BY) license (<https://creativecommons.org/licenses/by/4.0/>).

chemical species due to the weak molecule-surface interactions? In this mini-review, we have selected a few recent articles describing some innovative solutions to achieve on-surface chemistry on inert surfaces.

2. Results

2.1. Passivated-metal surface

2.1.1. Light-induced reactions

Light-induced reactions on inert surfaces are very promising because this type of reaction does not necessarily require substrate electrons. The kinetics and the thermodynamics of the photochemical transformation can be controlled precisely by means of the duration, the intensity, and the energy of the illumination [26]. From the point of view of on-surface synthesis, light-induced reactions occur in two approaches: (1) the formation of photo-generated reactive species with a sufficient lifetime to diffuse on surfaces and react with other un- or activated species or (2) a direct photochemical linking, based on the photoexcitation of one precursor which then reacts with an adjacent molecule to lead to a covalently bound ground state via a relaxation. In this latter case, the molecules have to be pre-organized in the right manner to efficiently couple adjacent monomers to give defect-free nanostructures.

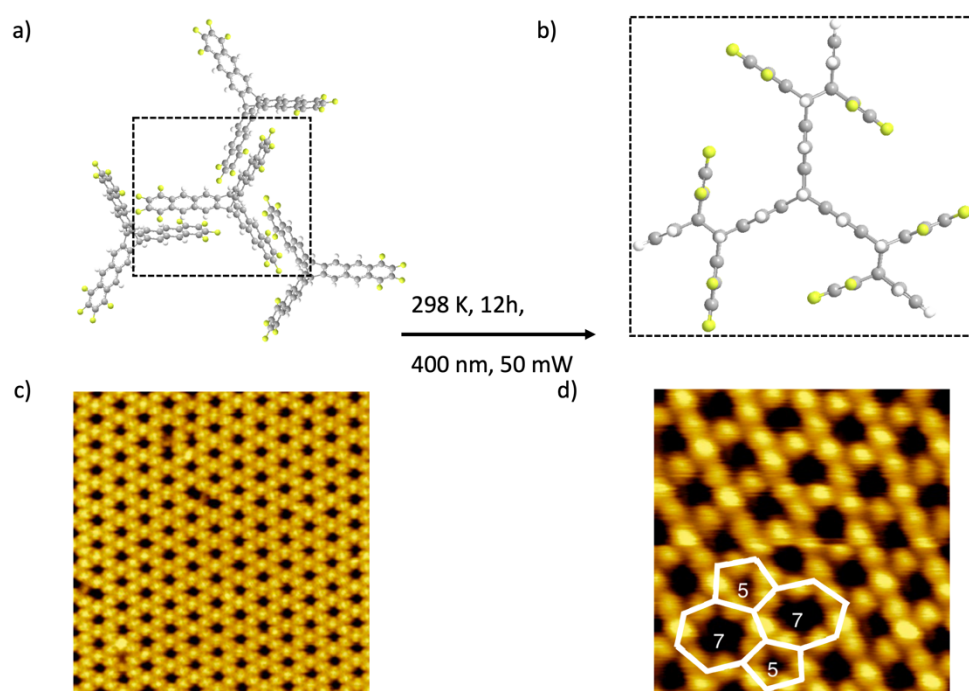


Figure 1. a) Top view of self-assembled fantrip molecules due to π - π interactions. b) 2D covalent network obtained by a [4+4] cycloadditions of adjacent fantrip molecules. c) STM image after deposition of fantrip onto hexacosane-passivated graphite following by a thermal annealing at 353 K ($V_s = -3.2$ V, $I_t = 3$ pA, 298K, 22×22 nm²). d) STM image obtained after UV-light illumination ($V_s = -3.0$ V, $I_t = 3$ pA, 298 K, 9×9 nm²). The covalently bounded 2D-network is constituted mainly by hexagons with a minor presence of pentagons and heptagons (highlighted by white polygons).

An illustrative example of the second approach is the work done Grossmann *et al.* The authors investigate the on-surface formation of extended 2D-polymers by using STM-UHV [27]. They chose fantrip molecules, which is a fluorinated anthracene triptycene (Figure 1a), as monomer. Indeed, fantrip molecules are known to efficiently photopolymerize in the crystal state through a [4+4] cycloaddition reaction [28]. As non-metallic surface, they chose a passivated graphite surface, obtained by deposition of a monolayer of hexacosane molecules ($C_{26}H_{54}$). This decoupling layer is mandatory to assume the required pre-organization of monomers. In a next step, fantrip molecules were deposited onto the adlayer of hexacosane molecules. STM images show formation of highly-organized 2D extended supramolecular network with the requested face-to-face arrangement of all adjacent fantrip molecules. After illumination at 400 nm with a power of 50 mW during 56h, the starting supramolecular network is converted into a new continuous hexagonal network. The resulting covalent network is well organized, few defects, corresponding to pentagons or heptagons instead of hexagons, are rarely observed. By using STM images and local Fourier-transform infrared spectroscopy (nano-FTIR), the photopolymerization was fully demonstrated. This method is very interesting to reach on-surface 2D-polymers. However, this strategy is not suitable for conjugated 2D-polymers, each [4+4] cycloaddition reaction leading to unconjugated nodes between monomers.

2.1.2. On-flight activated reactions

A general procedure for the synthesis of conjugated polymers by direct C-C bond coupling onto inert surfaces remains challenging, despite of many attempts. Instead of introducing an external stimulus to circumvent the lack of a chemical contribution from inert substrate due to the absence of electronic states in the respective energy window, Galeotti *et al.* propose an innovative solution [29]. Thanks to a deep analysis of the literature, they combined two contributions: (1) organic radicals can be deposited onto a surface and then react with pre-adsorbed monomers [30] and (2) deiodination of iodophenyl molecules occurs at room temperature on an Au(111) surface [31]. Therefore, they propose to deposit terphenyl radicals previously generated by a radical deposition source onto two passivated surfaces, Au(111)-I and Ag(111)-I surfaces [32, 33] in UHV. These two surfaces are obtained by chemisorption of a iodine monolayer, acting as a passivating layer, onto, respectively, Au(111) and Ag(111) surfaces. The iodine adlayer assumes the passivation of the underlying metal surfaces. This radical deposition source is constituted by a heated (500 K) gold-plated stainless-steel tube. The molecules undergo a lot of adsorption/desorption steps in the tube, leading to the formation of expected terphenyl radicals (Figure 2a).

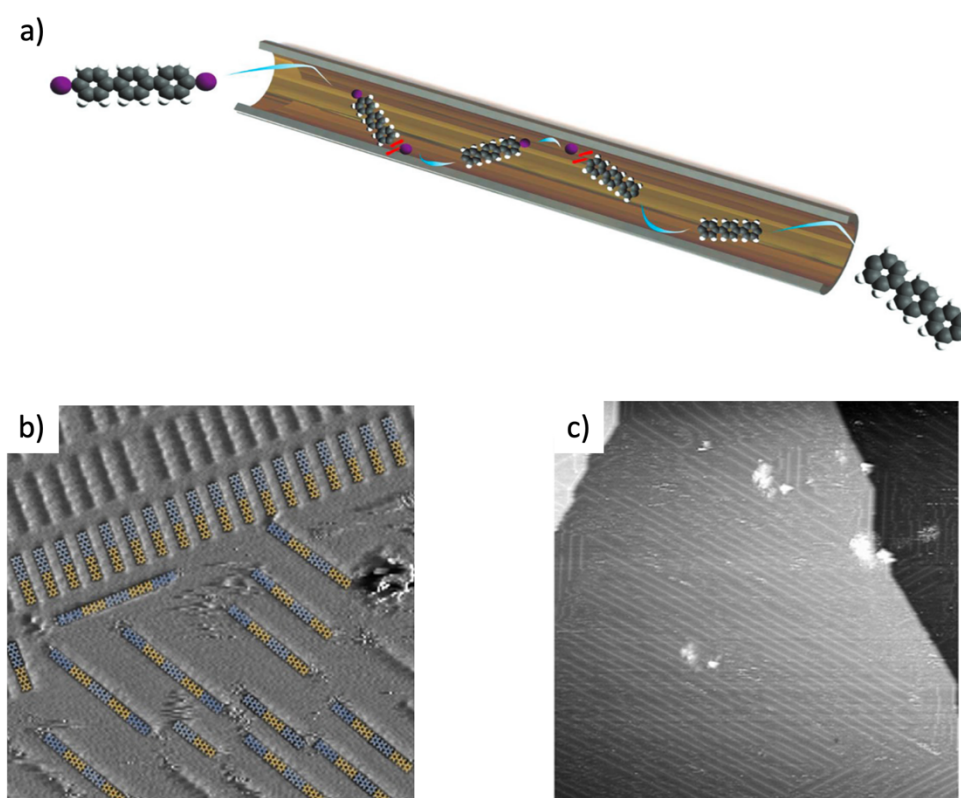


Figure 2. a) Scheme of principle of direct deposition of organic radicals by activation during the time-of-flight of iodinated precursors passing through a gold-plated stainless steel drift tube. b) STM image after deposition of triphenyl diradicals and a thermal annealing at 375 K ($V_s = -0.96$ V, $I_t = 104$ pA, 5K, 30×30 nm²) onto Au(111)-I surface. c) STM image after deposition of triphenyl diradicals and a thermal annealing at 425 K ($V_s = -1.19$ V, $I_t = 84$ pA, 5K, 100×100 nm²).

Then, radicals are deposited on passivated surface, held at room temperature. The rod-like structures observed in STM images are attributed to sexiphenyl, which originates from the dimerization of terphenyl radicals. If the surface is then annealed at 375 K, some longer oligophenylenes are observed. This observation clearly demonstrates that terphenyl radicals are stable and diffuse on Ag(111)-I and Au(111)-I surfaces, even upon mild thermal annealing. The RDS method seems to be a very efficient way to induce radical polymerization on passivated surfaces.

2.1.3. STM tip activated reactions

On-surface synthesis under ultrahigh-vacuum (UHV) conditions has attracted considerable attention to generate new and stable molecular structures that are sometimes impossible to address by using standard synthetic procedures, due to the confinement of molecules onto surfaces [34] or to the induction of reaction by the injection tunneling electrons with an atomic precision [35]. In this context, Kaiser *et al.* investigated the on-surface synthesis of a cyclo[18]carbon [36] by using STM-UHV and AFM-UHV. Indeed, cyclo[n]carbons are a family of carbon allotropes. They have been widely simulated because they have unique electronic properties. According to the literature, the prediction of these electronic properties is strongly dependent of the employed method of simulation, leading to an intense theoretical debate [37,38]. In order to determine the best method of simulation to address these electronic properties, many attempts of cyclo[n]carbons synthesis were done, following the conventional chemistry methods, for the purpose of experimentally probing their electronic properties. The most powerful strategy is based on a masked

alkyne equivalent incorporated into a cyclic precursor designed to generate cyclo[n]carbon when activated by heat or light. Despite many efforts, this type of carbon allotrope being too reactive was impossible to isolate [39].

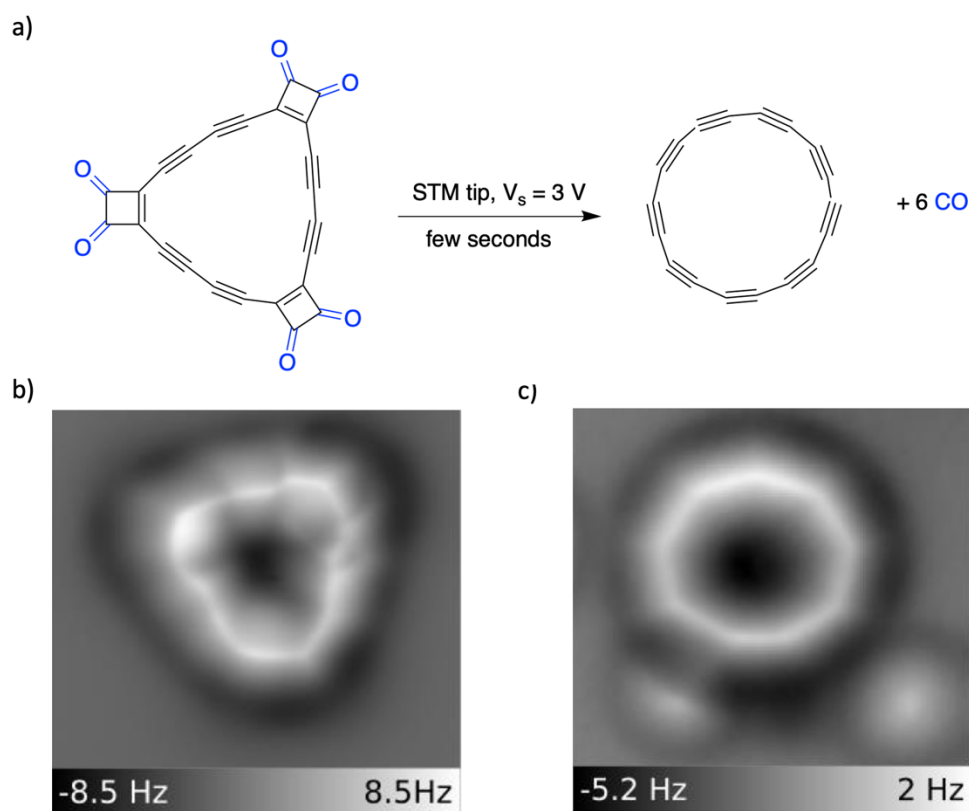


Figure 3. a) Synthesis of cyclo[18]carbon by using STM tip to inject electrons and induce decarbonylation of cyclocarbon oxide adsorbed onto a NaCl bilayer deposited on Cu(111). b) AFM image of cyclocarbon oxide at 5K. c) AFM image of cyclo[18]carbon at 5 K.

Alternatively, in the context of on-surface chemistry, the cyclo[18]carbon molecules are accessible through the decarbonylation reaction of corresponding cyclocarbon oxide [40]. Kaiser *et al.* proposed to generate on a surface the cyclo[18]carbon by using cyclocarbon oxide which are more stable than cyclo[18]carbon [36]. To reinforce the stability of both precursor and expected product, they deposited cyclocarbon oxide on a Cu(111) partially covered with (100) oriented bilayer of NaCl held at 10 K. Each CO function was removed by placing the STM tip in the vicinity of the molecule and by increasing the sample bias voltage to 3 V for a few seconds. This multi-step procedure led to the formation of expected cyclo[18]carbon molecules and 6 CO molecules adsorbed on the underlying surface (Figure 3a) as confirmed by nc-AFM performed at 5 K. Despite a long procedure and a global yield of conversion of 13%, this method demonstrates the unique ability of on-surface chemistry to investigate some molecules which are impossible to address by conventional synthetic method. Despite the fact that, this method is only limited to the transformation of a few molecules unlike other methods (light, thermal annealing) used in on-surface chemistry, it allows high precision control over the reaction at the molecular scale

2.2. Semiconductors

2.2.1. Silicon surfaces

The development of on-surface chemistry on a silicon surface is still a major scientific challenge with an industrial impact because silicon wafers are commonly used in electronic devices. Silicon crystals have a diamond structure, *i.e.* the atoms are sp^3 hybridized and bonded to four nearest neighbors in tetrahedral coordination. Consequently, when the crystal is cut or cleaved, Si-Si bonds are broken, creating dangling bonds at the surface [41]. These dangling bonds are the source of the surface chemical activity of silicon surfaces [42]. The strong molecule-substrate interactions can decompose molecules or disrupt the diffusion of precursors onto the surface, which prevents the formation of polymeric nanostructures.

The Si(001)-(2x1):H surface is one of the first silicon surfaces which was investigated because the hydrogen layer insures the decoupling of the molecules from the silicon substrate avoiding the alteration of the electronic structure of the molecules. In their work, Eisenhut *et al.* used this passivated surface to synthesize on-surface long acene molecules, a very important class of molecule for molecular electronics and spintronics [43].

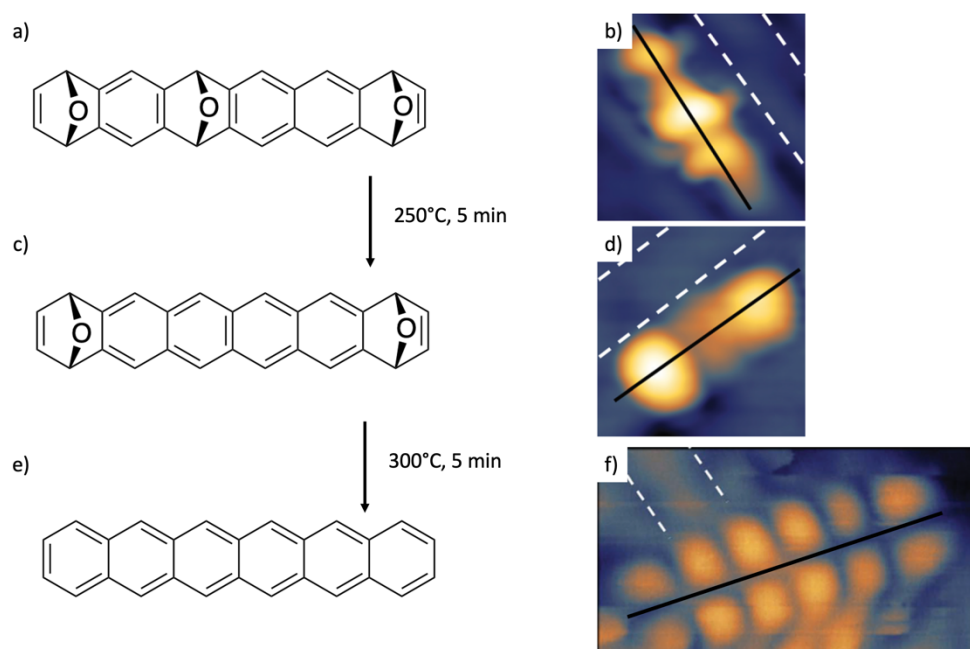


Figure 4. a) Triepoxyhexacene (Hn3O) molecules, b) STM image ($V_s = -2.0$ V, $I_t = 50$ pA, 5K, 2.5×2.5 nm²) of Hn3O. c) diethoxyhexacene (Hn2O) molecules obtained after a thermal annealing of Hn3O and d) corresponding STM image ($V_s = -3.0$ V, $I_t = 15$ pA, 5K, 2.5×2.5 nm²). e) Hexacene molecules obtained after a thermal annealing of Hn2O, and f) STM images ($V_s = -3.5$ V, $I_t = 15$ pA, 5K, 8×2 nm²). All STM images are obtained on a Si(001)-(2x1):H surface. The white dashed lines indicate the dimer row direction and the black line shows the direction of the investigated molecule.

If long acenes are very promising due to their unique electronic properties, for instance they can be considered as they constitute the narrowest zigzag graphene nanoribbons with potential application in spintronics [44]. Their synthesis is still challenging due to their lack of stability and solubility [45]. One of the efficient ways to circumvent these problems is to proceed through an on-surface chemical reaction using an appropriate acene precursor [46]. Eisenhut *et al.* have investigated this strategy on a Si(001)-(2x1):H surface by using STM-UHV to achieve the on-surface synthesis of hexacene on this passivated silicon surface [43]. From the point of view of synthetic chemistry, the long acenes

are usually obtained by multi-step iterative procedure, including several aryne cycloadditions [46]. These aryne cycloadditions lead to the formation of bicyclic compounds with several epoxycycles (Figure 4a). This triepoxyhexacene molecule was deposited onto Si(001)-(2x1) : H surface by standard sublimation procedure in UHV (Figure 4b). After thermal annealing, the triepoxyhexacene molecule was fully deoxygenated to give the hexacene molecules (Figure 4e-f). These deoxygenative steps are very efficient on Si(001)-(2x1) : H surface due to the strong Si-O interaction as highlighted by DFT simulation. These DFT simulations show that the oxygen atoms of triepoxyhexacene molecule are pointed to the surface, promoting the C-O bond cleavage and the formation of Si-O bonds. Scanning tunneling spectroscopy of hexacene molecules has been also performed, showing that the electronic properties of hexacene molecules are decoupled from the underlying surface. This work demonstrates that on-surface chemistry on Si(001)-(2x1) : H surface can be used to investigate the electronic properties of an in-situ generated molecule, opening the way for molecular electronics or spintronic on a silicon surface.

To circumvent the problem of silicon surface reactivity with organic molecules, the Si(111)-B $\sqrt{3}\times\sqrt{3}$ R30° surface has been used as a substrate. This surface possesses the unique particularity to show depopulated dangling bonds due to the presence of boron atoms underneath the top silicon layer [47]. The surface has been widely used to achieve the formation of extended 2D-supramolecular networks [48]. However, this strategy strongly limits the ability of the electrons to be involved in a chemical reaction between adsorbed molecules.

Therefore, Geagea *et al.* propose to use the tunnel-electron of the STM junction in order to induce a chemical reaction on a Si(111)-B $\sqrt{3}\times\sqrt{3}$ R30° surface in UHV [49]. The authors investigate the ability of an STM-tip to generate an organic radical and initiate a free radical polymerization process, with both steps occurring on the chosen semiconductor surface.

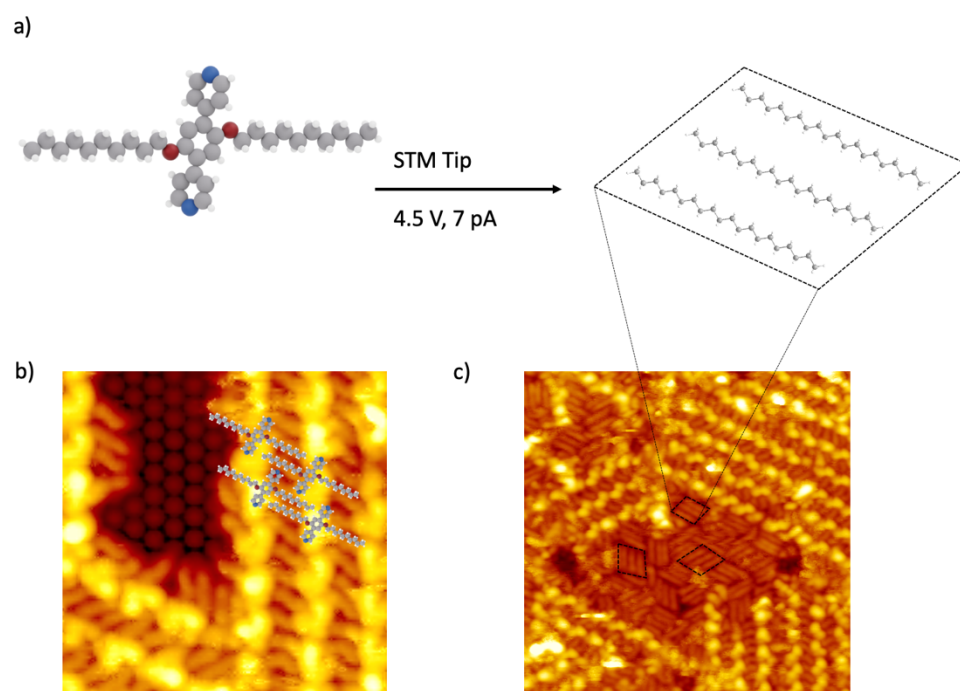


Figure 5. a) Chemical pathway for the STM tip-induced transformation of 1,4-bis(pyridyl)-2,5-bis(decyloxy)benzene (PDB-OC10) molecules into C₂₀ alkanes on the Si(111)-B surface. b) STM image ($V_s = -1.3$ V, $I_t = 7$ pA, 110 K, 10×10 nm²) of the supramolecular network constituted by PDB-OC10 molecules on Si(111)-B surface, with the corresponding model. c) STM image ($V_s = -1.3$ V, $I_t = 7$ pA, 110 K, 10×10 nm²) of the C₂₀ alkanes on the Si(111)-B surface, with the corresponding model.

7 pA, 110 K, 25 x 25 nm²) of a uncovered area of the previously observed supramolecular network of PDB-OC10 molecules fully filled with rod-like structures released by STM tip during scanning. These rod-like structures are attributed to C₂₀ alkanes.

The designed molecule, 4-bis(pyridyl)-2,5-bis(decyloxy)benzene (PDB-OC10), for this study is an aryl alkyl ether derivative since the electrochemical behavior of this type of molecule has been studied and shown that can undergo the formation of phenoxide anions and alkyl radicals via one-electron reduction process (Figure 5a) [50]. In addition, it can be engineered to reinforce molecule surface interactions by adding pyridyl moieties to the aryl based core and promote stable linear arrangements on Si(111)-B $\sqrt{3}\times\sqrt{3}$ R30° surface allowing more precise control while attempting to activate molecule by STM tip (Figure 5b).

Thanks to a deep voltage-dependency analysis, the authors found that at a voltage of -4.5 V, the dissociation of the PDB-OC10 molecule into phenoxide derivative and alkyl radical was done successfully through a dissociative electron attachment mechanism despite the absence of any catalytic assistance of the surface. The resulting alkyl radicals were stored and then released from the STM tip on the surface. These alkyl radicals react to form longer alkane derivatives, from dimer to hexamer, through a radical oligomerization process (Figure 5c). Indeed, the formation of long alkanes is explained by the chain reaction. The initiation step is the activation by a dissociative electron attachment. The propagation is the hydrogen atom transfer reaction of an alkyl radical with another alkane, leading to a longer alkyl radical. Finally, radical oligomerization is ended by the reaction between two radicals [49].

To sum up, on-surface chemistry was successfully achieved on a silicon surface by using tunnel electron(s) to dissociate a molecule through a dissociative electron attachment mechanism despite absence of any catalytic assistance of the surface. In addition, collective production, as well as controlled number of radicals, are possible due to the STM tip, playing a key role in stabilizing and transferring the reactive species. Consequently, the amount of radical desired can be produced, stocked, and then transferred with high precision by STM tip. Once released on the surface, alkyl radicals polymerized to give longer alkane derivatives by a radical reaction. Due to the confinement on the surface, the oligomer products possess a linear conformation (no cross polymerization like in solution) that can be attributed to selective diffusion paths of the reactive species on Si(111)-B surface.

2.2.2. Non-silicon based semiconductors

As described in the introduction, recent progress in the field of on-surface chemistry is driven by the construction of complex molecular architectures via surface-assisted C–C coupling on single-crystal metal surfaces (mainly Ag(111), Cu(111) and Au(111) surfaces) [4–8]. The cleavage of C–Br bonds and C–H bond of polyaromatic followed by formation of C–C bonds led to atomically precise nanographenes and nanoribbons [11]. Iodine and chlorine atoms were also used on metal surfaces. The properties of C–F bonds are quite different from other carbon-halogen bonds and paves the way toward a proper on-surface fluorine chemistry [51,52]. Amsharov used these unique properties to successfully achieve the cyclodehydrofluorination of fluoarenes on bulk metal oxides. He found that Al₂O₃, TiO₂, In₂O₃ and ZrO₂ are the most active oxides in cyclodehydrofluorination reactions. He also proposed a mechanism for metal oxide mediated intramolecular cyclization via HF elimination [53]. On the basis of his work, he then investigated the ability of this strategy to give carbon nanostructures in a fully controllable manner directly on insulating metal oxide surfaces.

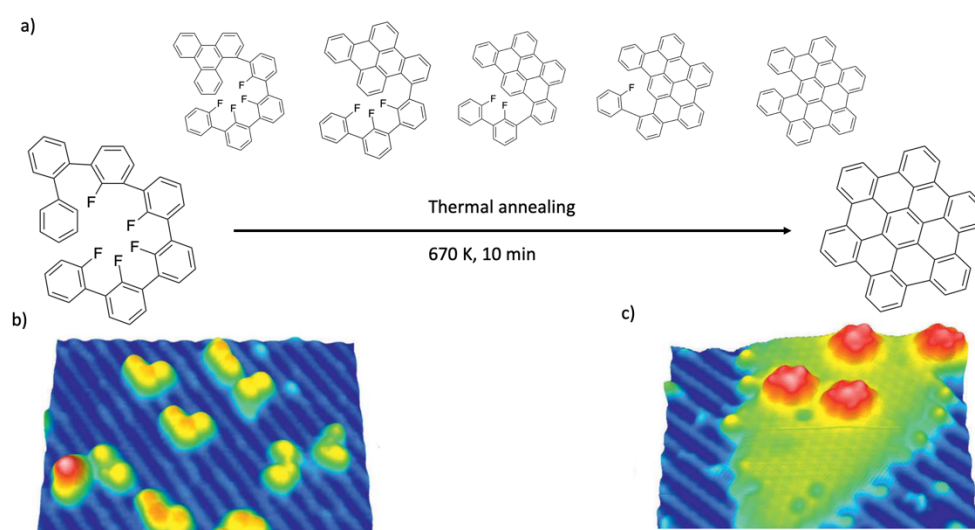


Figure 6. a) Chemical pathway for the thermal-induced transformation of dibenzo[j,k,rst]phenanthro[9,10,1,2-defg]pentaphene (DBPP) into hexabenzocoronene (HBC) on the rutile $\text{TiO}_2(011)\text{-}2\times 1$ surface. b) STM image ($V_s = 2.0$ V, $I_t = 10$ pA, 298 K, 13×10 nm²). c) STM image ($V_s = 2.5$ V, $I_t = 50$ pA, 298 K, 9×7 nm²) of HBC molecules obtained after a thermal annealing of DBPP molecules.

Kolmer *et al.* began by the investigation of intramolecular cyclodehydrofluorination on rutile TiO_2 surface by using STM-UHV [54]. In order to demonstrate the ability of their method to give nanographene, they chose to synthesize the hexabenzob[bc,ef,hi,kl,no,qr]coronene (HBC), an archetype of nanographene molecule, which has been efficiently obtained in UHV conditions on Cu(111) surface [55]. One of the key-points of the programmed cyclodehydrofluorination is the close proximity of C-F and C-F targeted bonds. This was assumed thanks to the smart design of molecular precursor (Figure 6a). However, after deposition on the rutile (011) surface, the molecular precursors adopt several geometries due to the flexibility of the substituents. Despite of this observation, the thermal annealing (10 min, 670 K) led to the formation of expected HBC molecules. This result demonstrated the cyclodehydrofluorination reaction on a rutile TiO_2 surface. In addition, the observation of the last intermediate (those with two remaining hydrogen atoms, Figure 6a) indicates that, on the TiO_2 surface, the cyclodehydrogenation is possible but it is the limiting step of the process, with a higher activation barrier than cyclodehydrofluorination reaction [54].

This work represents very important starting point for the growth of graphene nanoribbons on metal oxide surfaces. However, the lack of catalytic activity of the metal oxide surface demands alternatives for the cyclodehydrogenation reaction, which is required to give the expected graphene nanoribbons.

Correspondingly, Kolmer *et al.* proposed one year later, an efficient way to elaborate graphene nanoribbons on rutile $\text{TiO}_2(011)$ surface [56]. The synthesized a molecular precursor, 10,10''-dibromo-1',4'-difluoro-9,9':10',9''-teranthracene, including three anthracenyl moieties, which is the carbon-based skeleton of GNR, two bromine atoms for the growth of the main axis of the GNR and two fluorine atoms in order to promote the aromatization required for the formation of the expected GNR (Figure 7a).

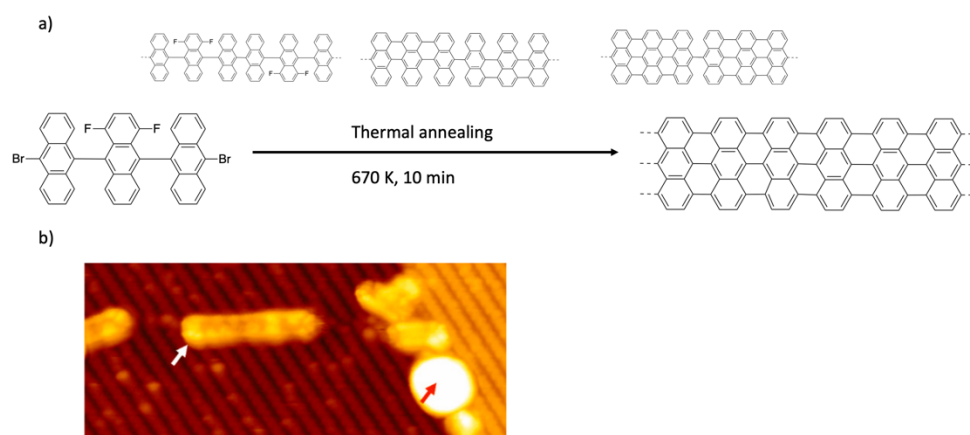


Figure 7. a) Chemical pathway for the thermal-induced polymerization of 10,10''-dibromo-1',4'-difluoro-9,9':10',9''-teranthracene (DBDFTA) into 7-armchair graphene nanoribbon on the rutile TiO₂(011)-2x1 surface. b) STM image ($V_s = 2.5$ V, $I_t = 10$ pA, 298 K, 13×6 nm²) of 7-armchair graphene nanoribbon (highlighted with a white arrow) obtained after a thermal annealing of DBDFTA molecules. Thermal annealing leads also to the formation of side-products, as shown with the red arrow.

A thermal annealing (10 min, 670 K) led to the formation of elongated nanostructures adsorbed on the rutile surface. Electronic properties, determined by scanning tunneling spectroscopy in UHV and lateral manipulation, are in good agreement with the on-surface synthesis of GNRs. By comparison to those obtained on metal surfaces, these nanoribbons are shorter (below 10 nm) but their interaction with the (TiO₂) substrate electrons is very weak because the quasi-particle gap is close to the value expected for the free-standing GNR.

To sum up, highly selective and sequential activations of C-Br, C-F bonds, and cyclodehydrogenation are efficient on the TiO₂ surface and could constitute a very promising way to elaborate atomically precise carbon nanostructures on other semi-conductors.

2.3. Bulk Insulators

A major challenge for future device fabrication consists in the development of on-surface chemistry onto bulk insulator surfaces, because it is mandatory to decouple the electronic structure of the functional organic nanostructures from those of the underlying surface. However, if the band gap of the bulk insulators is very interesting in terms of electronic decoupling, it also strongly alters the ability of these surfaces to be involved in the chemical synthesis. Therefore, adapted external stimuli are required to induce the chemical transformation of adsorbed molecules into new compounds.

2.3.1. Thermal-induced polymerization

In their work, Richter *et al.* investigated the thermal-induced polymerization of a diacetylene derivative on the calcite (10.4) surface by using AFM-UHV [57]. Diacetylene molecules are based on the alternance of two carbon-carbon triple bonds, which can be efficiently polymerized into the corresponding diacetylene polymerized chain, one of the seminal conductive polymers [58]. This polymerization has been previously investigated on different kinds of surface [59,60], except on bulk insulators.

To achieve the polymerization on a (10.4) calcite surface, the authors designed a molecule based on a diacetylene core surrounded by two carboxylic functional groups (Figure 8a). As the (10.4) calcite surface is ionic, the molecules are H-bonded onto the surface thanks to the hydrogen bonds between COOH-moieties of molecules and calcite carbonate of the surface. This molecule-surface interaction being very strong, the resulting

supramolecular network is commensurable with the surface, with a (1x3) superstructure (Figure 8b), as demonstrated by means of AFM images in UHV and DFT simulations.

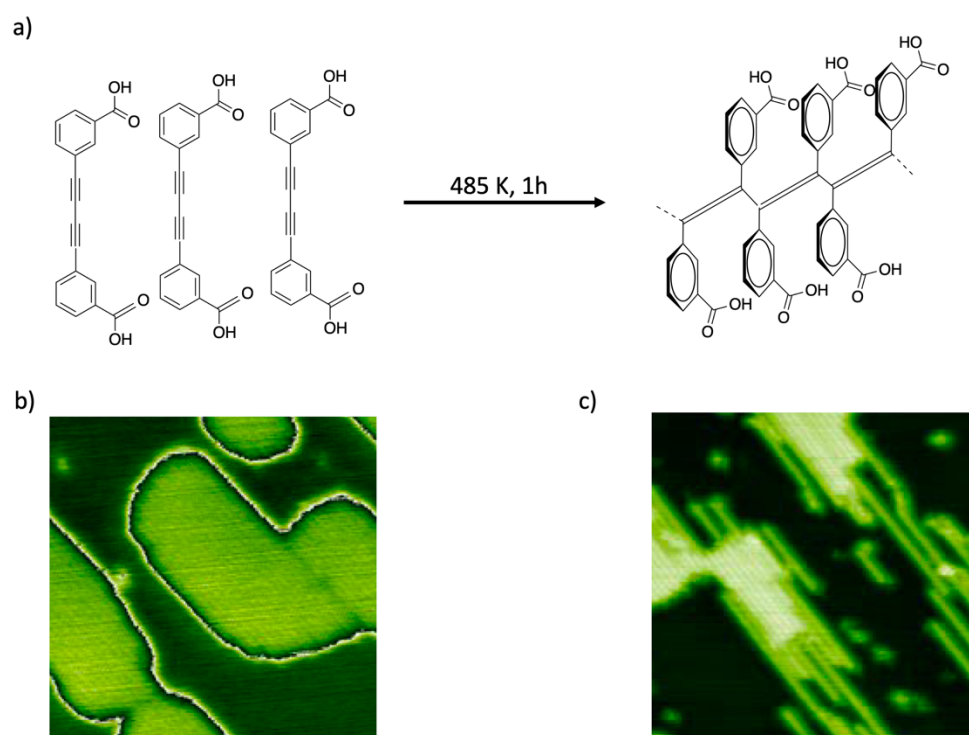


Figure 8. a) Chemical pathway for the thermal-induced polymerization of 3,3'-(1,3-butadiyne-1,4-diyl)bisbenzoic acid into a poly(substituted)diacetylene chains. b) AFM image (50 x 50 nm²) of self-assembled 3,3'-(1,3-butadiyne-1,4-diyl)bisbenzoic acid molecules on the calcite (10.4) c) AFM image (50 x 50 nm²) recorded after thermal annealing of 3,3'-(1,3-butadiyne-1,4-diyl)bisbenzoic acid molecules.

In this supramolecular network, the carbon-carbon triple bonds of adjacent molecules are perfectly aligned along the calcite [010] axis, which is required to achieve the polymerization of these triple bonds. After thermal annealing at 485 K during 1h, the features observed in the AFM images have been strongly modified (Figure 8c). Instead of compact islands, single bright stripes still oriented along the calcite [010] axis are observed. The periodicity inside each bright line is of 0.5 nm. All the observations support that the initial supramolecular networks have been transformed into the corresponding 1D diacetylene polymerized chain due to the thermally-induced reaction between carbon-carbon triple bonds. The resulting 1D chains of polymer are still oriented to the calcite [010] axis, because of the electrostatic interaction of carboxylic groups with the underlying ionic surface. In addition, the 1D chains of polymer are stable on the surface for several days when they are stored at room temperature in UHV.

This method leads to the formation on 1D-conductive polymers carried out on a bulk insulator surface. The key-point is the pre-organization of monomers in supramolecular networks in a periodic arrangement, which is in agreement with the polymerization of carbon-carbon triple bonds of adjacent molecules. This is due to strong molecule-surface interaction. However, if this strong interaction is an advantage to assume the formation of stable polymers, it is detrimental to the formation of long polymer chains because the diffusion of molecular precursors is strongly inhibited by this interaction. This is the main reason for justifying the formation of polymers with a length below 60 nm. Therefore, the development of other strategies to increase the length of polymers is required.

2.3.2. Light-induced polymerization

As mentioned previously, light-induced reactions are a convenient way to circumvent the lack of reactivity of passivated surfaces. In their work, Para *et al.* combine the advantages of side-product-free photochemistry, efficient template effect of insulating substrate, and for the first time, a radical chain reaction [61]. This unique combination leads to the formation of 1D-polymers with a defect-free structure of up to 10'000 molecules (1 μm in length). Each of these parameter plays an important role to achieve this polymerization.

After deposition of dimaleimide molecules onto KCl(100) surface in UHV, the molecules diffuse over several hours on this ionic surface kept at room temperature and form a two-dimensional gas phase before slowly dewetting into larger multilayer crystallites. Biradical monomers are formed upon UV illumination due to homolytic photo-cleavage of the C=C bond of one of the two maleimide rings. As long as unexcited monomer precursors diffuse on the surface, they can react with the UV-generated biradical monomers to form a biradical dimer by chain-growth process until the formation of the ultra-long fibres (Figure 9a). The structure of the fibres formed is very regular and well oriented along the crystallographic axes of the KCl (100) substrate, as investigated by AFM, which indicates that the fibres are defect-free over large distances (Figure 9b). This is supported by the interaction of ionic substrate (KCl(100)) and properly chosen polar end groups (C=O). This interaction is involved in the growth of the 1D covalent fibers along a well-defined direction of the ionic substrate (Figure 9c), but also in the formation a 2D diluted gas phase of precursor molecules on the substrate surface at room temperature.

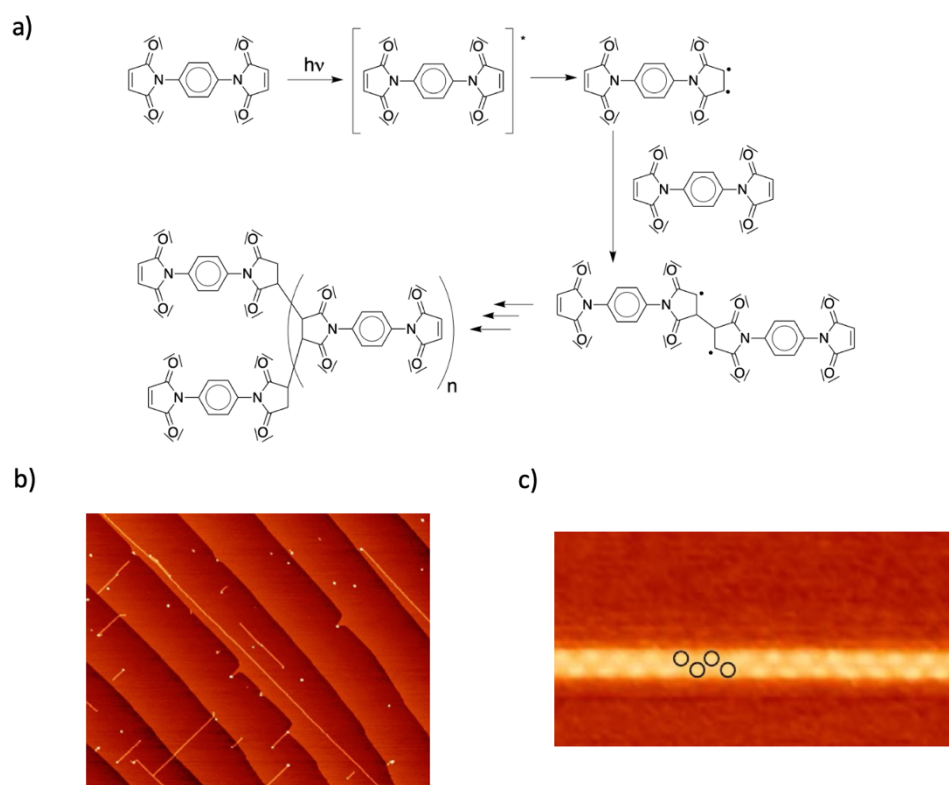


Figure 9. a) Chemical pathway for the light-induced polymerization of *N,N'*-(1,4-phenylene)dimaleimide into a poly(*N*-substituted)dimaleimide chains. b) AFM image (1000 x 1000 nm²) of a long fibres of poly(*N*-substituted)dimaleimide on a KCl(001) surface. c) Zoom of b) (20 x 10 nm²) showing a

zig-zag structure. This reflects a topological rumpling of the fibre due to a coincidence of every fifth molecule with the fourth cation along the KCl(001) crystal axis

Photo-induced radical chain polymerization is a very efficient method to generate large-extended, defect-free polymer fibres on insulating substrates. The two key parameters to increase the size of the resulting structure are (i) the UV-light intensity (number of nucleation sites created), and (ii) the tuning of molecule-surface interaction to control the diffusion of monomers and template effect of the substrate.

4. Conclusions

On-surface synthesis provides new possibilities to form highly-stable and atomically-defined nano-structures that exhibit desired electronic, optical, catalytic, and other properties. The spatial confinement of on-surface reactions gives access to entirely new reaction pathways and allows to guide the size, the shape, and the nature of the formed structures. The challenge one has to accept to overcome the limitations of low quality (extension and number of defects) and inhibited functionalities when using metal substrates is complex. A simple transition of the already well-known reactions which work on metal substrates to passivated substrates is impossible since on passivated substrates, the catalytic effect of the metal substrate is absent and the relatively high annealing temperatures applicable on metals cannot be used on passivated substrates due to the relatively low molecule-substrate interaction, which results in the desorption of molecules instead of the bond formation. Therefore, many outstanding results have been recently obtained in the field of on-surface chemistry onto inert surfaces. Covalently bonded nanostructures are accessible by combining the smart design of precursors and external stimuli (light, electrons and annealing) for each type of passivated surfaces.

Furthermore, the development of new analytical methods to fully describe on-surface reactions could be a possible route for advancing the field in the future. Indeed, despite their ability to resolve internal bonding structure, the bottleneck to fully characterizing the on-surface reactions is that STM or AFM are chemically insensitive. To overcome this lack of information, techniques such as infrared (IR) coupled with the AFM and Tip-Enhanced Raman Spectroscopy (TERS) to perform Raman spectroscopy on the nanometer scale could greatly improve on-surface chemistry studies in UHV, in the upcoming days. Finally, we believe that the current efforts carried out by the surface synthesis community will increase in order to improve the techniques for the synthesis of covalent nanostructures on low-reactive surfaces and demonstrate their importance in terms of applications to incorporate into future technologies.

Author Contributions: Writing-review and editing, E.G., F.P. and F.C.

Funding: This research was funded by “Agence Nationale de la Recherche, grant number OVA-TION ANR-19-CE09-0020, HITS ANR-20-CE09-0016, and Light4net ANR-21-CE09-0004” and “Pays de Montbéliard Agglomération”.

Data Availability Statement: Not applicable.

Acknowledgments: The authors thank Pr. Dr. C. Loppacher (IM2NP, Marseille), Pr. Dr. C. M. Thomas (IRCP, Paris) and Pr. Dr. A. Rochefort (Polytechnique Montréal) for fruitful discussions.

Conflicts of Interest: The authors declare no conflict of interest.

References

- Grill, L.; Dyer, M.; Lafferentz, L.; Persson, M. V.; Hecht, S. Nano-Architectures by Covalent Assembly of Molecular Building Blocks. *Nat. Nanotech.* **2007**, *2*, 687–691. DOI: 10.1038/nnano.2007.346
- Cai, L.; Ruffieux, P.; Jaafar, R.; Bieri, M.; Braun, T.; Blankenburg, M.; Seitsonen, A. P.; Saleh, M.; Feng, X.; Mullen, K.; Fasel, R. Atomically Precise Bottom-Up Fabrication of Graphene Nanoribbons. *Nature* **2010**, *466*, 470–473. DOI: 10.1038/nature09211
- Matena, M.; Riehm, T.; Stöhr, M.; Jung, T. A.; Gade, L. H. Transforming Surface Coordination Polymers into Covalent Surface Polymers: Linked Polycondensed Aromatics through Oligomerization of N-Heterocyclic Carbene Intermediates. *Angew. Chem. Int. Ed.* **2008**, *47*, 2414–2417. DOI: 10.1002/anie.200704072
- Grill, L.; Hecht, S. Covalent on-Surface Polymerization. *Nat. Chem.* **2020**, *12*, 115–130. doi:10.1038/s41557-019-0392-9.
- Clair, S.; de Oteyza, D. G. Controlling a Chemical Coupling Reaction on a Surface: Tools and Strategies for On-Surface Synthesis. *Chem. Rev.* **2019**, *119*, 4717–4776. DOI: 10.1021/acs.chemrev.8b00601
- Held, P. A.; Fuchs, H.; Studer, A. Covalent-Bond Formation via On-Surface Chemistry. *Chem. Eur. J.* **2017**, *23*, 5874–5892.
- Bartels, L. Tailoring Molecular Layers at Metal Surfaces. *Nat. Chem.* **2010**, *2*, 87–95. DOI: 10.1038/nchem.517
- Lackinger, M. On-Surface Polymerization - a Versatile Synthetic Route to Two-Dimensional Polymers: On-surface Polymerization. *Polym. Inter.* **2015**, *64*, 1073–1078. DOI: 10.1007/s10118-018-2070-6
- Geagea, E.; Jeannoutot, J.; Morgenthaler, L.; Lamare, S.; Rochefort, A.; Palmino, F.; Chérioux, F. Unravelling the Growth Mechanism of (3,1) Graphene Nanoribbons on a Cu(111) Surface. *Chem. Commun.* **2021**, *57*, 6043–6045. DOI: 10.1039/d1cc01173a
- Gomez-Herrero, A. C.; Sanchez-Sanchez, C.; Chérioux, F.; Martinez, J. I.; Abad, J.; Floreano, L.; Verdini, A.; Cossaro, A.; Mazaleyrat, E.; Guisnet, B.; Davide, P.; Lisi, S.; Martin Gago, J. A.; Coraux, J. Copper-Assisted Oxidation of Catechols into Quinone Derivatives. *Chem. Sci.* **2021**, *12*, 2257–2267. DOI: 10.1039/d0sc04883f
- Zuzak, R.; Jancarik, A.; Gourdon, A.; Szymonski, M.; Godlewski, S. On-Surface Synthesis with Atomic Hydrogen. *ACS Nano.* **2020**, *14*, 13316–13323. DOI: 10.1021/acsnano.0c05160
- Okawa, Y.; M. Aono. Nanoscale Control of Chain Polymerization. *Nature*, **2001**, *409*, 683–684. DOI: 10.1038/35055625
- Den Boer, D.; Elemans, J. A. A. W. Triggered Chemical Reactions by Scanning Tunneling Microscopy: From Atoms to Polymers. *European J. Polym.* **2016**, *83*, 390–406. DOI: 10.1016/j.eurpolymj.2016.03.002
- Fan, Q.; Martinez-Jimenez, D.; Krug, C. K.; Brechmann, L.; Kohlmeyer, C.; Hilt, G.; Hieringer, W.; Schirmeisen, A.; Gottfried, J. M. Nanoribbons with Nonalternant Topology from Fusion of Polyazulene: Carbon Allotropes beyond Graphene. *J. Am. Chem. Soc.* **2019**, *141*, 17713–17720. DOI: 10.1021/ja9b08060
- Shen, Q.; Gao, H.-Y.; Fuchs, H. Frontiers of on-surface synthesis: From principles to applications *Nano Today* **2017**, *13*, 77–96. DOI: 10.1016/j.nantod.2017.02.007
- Palmino, F.; Loppacher, C.; Chérioux, F.; Photochemistry Highlights on On-Surface Synthesis, *ChemPhysChem* **2019**, *20*, 2271–2280. DOI: 10.1002/cphc.201900312
- Basagni, A.; Ferrighi, L.; Cattelan, M.; Nicolas, L.; Handrup, K.; Vaghi, L.; Papagni, A.; Sedona, F.; Di Valentin, C.; Agnoli, S.; Sambì, M. On-surface photo-dissociation of C–Br bonds: towards room temperature Ullmann coupling. *Chem. Commun.* **2015**, *51*, 12593–12596. DOI: 10.1039/C5CC04317D
- Guan, L.; Palmino, F.; Lacroix, J.-C.; Chérioux, F.; Sun, X. [2+2] Cyclo-Addition Reactions for Efficient Polymerization on HOPG surface at ambient Conditions. *Nanomaterials* **2022**, *12*, 1334–1346. DOI: 10.3390/nano1281334
- Gross, L.; F.; Schuler, B.; Pavlicek, P.; Fatayer, S.; Majzik, Z.; Moll, N.; Pena, D.; Meyer, G. Atomic Force Microscopy for Molecular Structure Elucidation. *Angew. Chem. Int. Ed.* **2018**, *57*, 3888–3908. DOI: 10.1002/anie.201703509
- Wu, X.; Delbianco, M.; Anggara, K.; Michowicz, T.; Pardo-Vargas, A.; Bharate, P.; Sen, S.; Pristl, M.; Rauschenbach, S.; Schlick-hum, U.; Abb, S.; Seeberger, P. H.; Kern, K. Imaging single glycans. *Nature* **2020**, *582*, 375–378. DOI: 10.1038/s41586-020-2362-1
- Brülke, C.; Bauer, O.; Sokolowski, M. M. The influence of an interfacial hBN layer on the fluorescence of an organic molecule. *Beilstein J. Nanotechnol.* **2020**, *11*, 1663–1684. DOI: 10.3762/bjnano.11.149
- Jacobse, P. H.; Mangnus, M. J. J.; Zevenhuizen, S. J. M.; Swart, I. Mapping the Conductance of Electronically Decoupled Graphene Nanoribbons. *ACS Nano*, **2018**, *12*, 7048–7056. DOI: 10.1021/acsnano.8b02770
- Lackinger, M.; Synthesis on inert surfaces. *Dalton Trans.* **2021**, *50*, 10020–10027. DOI: 10.1039/d1dt00058f
- Sun, K.; Fang, Y.; Chi, L. On-surface synthesis on nonmetallic substrates. *ACS Materials Lett.* **2021**, *3*, 56–63. DOI: 10.1021/acsmaterialslett.0c00452
- Maier, S.; Stöhr, M. Molecular assemblies on surfaces: towards physical and electronic decoupling of organic molecules. *Beilstein J. Nanotechnol.* **2021**, *12*, 950–956. DOI: 10.3762/bjnano.12.71
- Palmino, F.; Loppacher, C.; Chérioux, F.; Photochemistry highlights on n-surface synthesis. *ChemPhysChem* **2019**, *20*, 2271–2280. DOI: 10.1002/cphc.201900312
- Grossmann, L.; King, B. T.; Reichlmaier, S.; Hartmann, N.; Rosen, J.; Heckl, W. M.; Bjork, J.; Lackinger, M. On-Surface Photopolymerization of Two-dimensional Polymers Ordered on the Mesoscale. *Nature Chem.* **2021**, *13*, 730–736. DOI: 10.1038/s41557-021-00709-y
- Kissel, P.; Murray, D. J.; Wulftrange, W. J.; Catalano, V. J.; King, B. T. A nanoporous two-dimensional polymer by single-crystal-to-single-crystal photopolymerization. *Nature Chem.* **2014**, *6*, 774–778.
- Galeotti, G.; Fritton, M.; Lackinger, M. Carbon-Carbon Coupling on Inert Surfaces by Deposition of En Route Generated Aryl Radicals. *Angew. Chem. Int. Ed.* **2020**, *59*, 22785–22789. DOI: 10.1002/anie.202010833

30. Lau, K. K. S.; Gleason, K. K. Initiated Chemical Vapor Deposition (iCVD) of Poly(alkyl acrylates): An Experimental Study. *Macromolecules* **2006**, *39*, 3688–3694. DOI: 10.1021/ma0601619
31. Eichhorn, J.; Nieckarz, D.; Ochs, O.; Debabrata, S.; Schmittl, M.; Szabelski, P. J.; Lackinger, M. On-Surface Ullmann Coupling: The Influence of Kinetic Reaction Parameters on the Morphology and Quality of Covalent Networks. *ACS Nano* **2014**, *8*, 7880–7889. DOI: 10.1021/nn501567p
32. Eder, G.; Smith, E. F.; Cebula, I.; Heckl, W. M.; Beton, P. H.; Lackinger, M. Solution Preparation of Two-Dimensional Covalently Linked Networks by Polymerization of 1,3,5-Tri(4-iodophenyl)benzene on Au(111). *ACS Nano*, **2013**, *7*, 3014–3021. DOI: 10.1021/nn400337v
33. Rastoo-Lahrood, A.; Bjork, J.; Lischka, M.; Eichhorn, J.; Kloft, S.; Fritton, M.; Samanta, D.; Schmittl, M.; Heckl, W. M.; Lackinger, M. post-synthetic Decoupling of On-surface Synthesized Covalent Nanostructures from Ag(111). *Angew. Chem. Int. Ed.* **2016**, *55*, 7650–7654. DOI: 10.1002/anie.201600684
34. Barth, J. V.; Constantini, G.; Kern, K. Engineering Atomic and molecular Nanostructures at Surfaces. *Nature* **2005**, *437*, 671–679. DOI: 10.1038/nature04166
35. Hla, S.-W.; Bartels, L.; Meyer, G.; Rieder, K.-H. Hla, S.-W.; Bartels, L.; Meyer, G.; Rieder, K.-H. Inducing All Steps of a Chemical Reaction with the Scanning Tunneling Microscope Tip: Towards Single Molecule Engineering. *Phys. Rev. Lett.* **2000**, *85*, 2777. DOI: 10.1103/PhysRevLett.85.2777
36. Kaiser, K.; Scriven, L. M.; Schulz, F.; Gawel, P.; Gross, L.; Anderson, H. L. An sp-Hybridized Molecular Carbon Allotrope, Cyclo[18]carbon. *Science* **2019**, *365*, 1299–1301. DOI: 10.1126/science.aay1914
37. Parasuk, V.; Almlof, J.; Feyereisen, M. W. The [18] all-carbon molecule: Cumulene or polyacetylene? *J. Am. Chem. Soc.* **1991**, *113*, 1040–1050. DOI: 10.1021/ja00003a052
38. Neiss, C.; Trushin, E.; Görling, A. The nature of one-dimensional carbon: Polyynic versus cumulenic. *ChemPhysChem* **2014**, *15*, 2497–2502. DOI: 10.1002/cphc.201402266
39. Diederich, F.; Rubin, Y.; Knobler, C. B.; Whetten, R. L.; Schriver, K. E.; Houk, K. N.; Li, Y. The higher oxides of carbon C_{8n}O_{2n} (n = 3–5): Synthesis, characterization, and X-ray crystal structure. Formation of cyclo[n]carbon ions C_n⁺ (n = 18, 24), C_n[–] (n = 18, 24, 30), and higher carbon ions including C₆₀⁺ in laser desorption Fourier transform mass spectrometric experiments. *J. Am. Chem. Soc.* **1991**, *113*, 495–500. DOI: 10.1021/ja00002a017
40. Rubin, Y.; Kahr, M.; Knobler, C. B.; Diederich, F.; Wilkins, C. L. All-carbon molecules: Evidence for the generation of cyclo[18]carbon from a stable organic precursor. *Science* **1989**, *245*, 1088–1090. DOI: 10.1126/science.245.4922.1088
41. Waltenburg, H. N.; Yates, J. T. Surface Chemistry of Silicon. *Chem. Rev.* **1995**, *95*, 1589–1673. DOI: 10.1021/cr00037a600
42. Hamers, R. J.; Wang, Y. Atomically-Resolved Studies of the Chemistry and Bonding at Silicon Surfaces. *Chem. Rev.* **1996**, *96*, 1261–1290. DOI: 10.1021/cr950213k
43. Eisenhut, F.; Krüger, J.; Skidin, D.; Nikipar, S.; Alonso, J. M.; Guitian, E.; Perez, D.; Ryndyl, D. A.; Pena, D.; Moresco, F.; Cuniberti, G. Hexacene generated on passivated silicon. *Nanoscale* **2018**, *10*, 12582–12587. DOI: 10.1039/c8nr03422b
44. Ruffieux, P.; Wang, S.; Yang, B.; Sanchez-Sanchez, C.; Liu, J.; Dienel, T.; Talirz, L.; Shinde, P.; Pignedoli, C. A.; Passerone, D.; Dumslaff, T.; Feng, X.; Mullen, K.; Fasel, R. On-surface synthesis of graphene nanoribbons with zigzag edge topology. *Nature* **2016**, *531*, 489 – 492. DOI: 10.1038/nature17151
45. Watanabe, M.; Chen, K.-Y.; Chang, Y. J.; Chow, T. J. Acenes Generated from Precursors and Their Semiconducting Properties. *Acc. Chem. Res.* **2013**, *46*, 1606–1615. DOI: 10.1021/ar400002y
46. Krüger, J.; Garcia, F.; Eisenhut, F.; Skidin, D.; Alonso, J. M.; Guitian, E.; Perez, D.; Cuniberti, G.; Moresco, F.; Pena, D. Decacene: On-Surface Generation. *Angew. Chem. Int. Ed.* **2017**, *56*, 11945–11948. DOI: 10.1002/anie.201706156
47. Lyo, I.-W.; Kaxiras, E.; Avouris, Ph. Adsorption of boron on Si(111): Its effect on surface electronic states and reconstruction. *Phys. Rev. Lett.* **1989**, *63*, 1261–1264. DOI: 10.1103/physrevlett.63.1261
48. Makoudi, Y.; Jeannoutot, J.; Palmino, F.; Chérioux, F.; Copie, G.; Krzeminski, C.; Cléri, F.; Grandidier, B. Supramolecular self-assembly on the B-Si(111)-(√3×√3)R30° surface: From Single Molecules to Multicomponent Networks. *Surf. Sci. Report* **2017**, *72*, 316–349. DOI: 10.1016/j.surfrep.2017.06.001
49. Geagea, E.; Jeannoutot, J.; Féron, M.; Palmino, F.; Thomas, C. M.; Rochefort, A.; Chérioux, F. Collective radical oligomerisation induced by an STM tip on a silicon surface. *Nanoscale* **2021**, *13*, 349–354. DOI: 10.1039/d0nr08291k
50. Koppang, M. D.; Woosley, N. F.; Bartak, D. E. Carbon-oxygen bond cleavage reactions by electron transfer. *J. Am. Chem. Soc.* **1984**, *106*, 2799–2805. DOI: 10.1021/ja00322a013
51. O'Hagan, D. Understanding organofluorine chemistry. An introduction to the C–F bond. *Chem. Soc. Rev.* **2008**, *37*, 308–319. DOI: 10.1039/b711844a
52. Clot, E.; Eisenstein, O.; Jasim, N.; MacGregor, S. A.; McGrady, J. E.; Perutz R.N. C-F and C-H Bond Activation of Fluorobenzenes and Fluoropyridines at Transition Metal Centers: How Fluorine Tips the Scales. *Acc. Chem. Res.* **2011**, *44*, 333–348. DOI: 10.1021/ar100136x
53. Amsharov, K. D. Cyclodehydrofluorination of fluoroarenes on metal oxides: Toward bottom-up synthesis of carbon nanostructures on insulating surfaces. *Phys. Status Solidi B* **2016**, *253*, 2473–2477. DOI: 10.1002/pssb.201600211
54. Kolmer, M.; Zuzak, R.; Steiner, A. K.; Zajac, L.; Englund, M.; Godlewski, S.; Szymonski, M.; Amsharov, K. Fluorine-programmed nanostructuring to tailored nanographenes on rutile TiO₂ surfaces. *Science* **2019**, *363*, 57–60. DOI: 10.1126/science.aav4954

55. Weiss, K.; Beernink, G.; Dötz, F.; Birkner, A.; Müllen, K.; Wöll, C. H. Template-Mediated Synthesis of Polycyclic Aromatic Hydrocarbons: Cyclodehydrogenation and Planarization of a Hexaphenylbenzene Derivative at a Copper Surface. *Angew. Chem. Int. Ed.* **1999**, *38*, 3748–3752. DOI: 10.1002/(SICI)1521-3773(19991216)38:24<3748::AID-ANIE3748>3.0.CO;2-0
56. Kolmer, M.; Steiner, A. K.; Izydorczyk, I.; Ko, W.; Engelund, M.; Szymonski, M.; Li, A.-P.; Amsharov, K. Rational synthesis of atomically precise graphene nanoribbons directly on metal oxide surfaces. *Science* **2020**, *369*, 571–575. DOI: 10.1126/science.abb8880
57. Richter, A.; Haapasilta, V.; Venturini, C.; Bechstein, R.; Gourdon, A.; Foster, A. S.; Kühnle, A. Diacetylene Polymerization on a Bulk Insulator Surface. *Phys. Chem. Chem. Phys.* **2017**, *19*, 15172–15176. DOI: 10.1039/C7CP01526G
58. Sakamoto, M.; Wasserman, B.; Dresselhaus, M. S.; Wnek, G. E. Enhanced electrical conductivity of polydiacetylene crystals by chemical doping and ion implantation. *J. Appl. Phys.* **1986**, *60*, 2799. DOI: 10.1063/1.337059
59. Okawa, Y.; Aono, M. Nanoscale control of chain polymerization. *Nature*, **2001**, *409*, 683–684. DOI: 10.1038/35055625
60. Deshpande, A.; Sham, C.-H.; Alaboson, J. M. P.; Mullin, J. M.; Schatz, G. C.; Hersam, M. C. Self-Assembly and Photopolymerization of Sub-2 nm One-Dimensional Organic Nanostructures on Graphene. *J. Am. Chem. Soc.* **2012**, *134*, 16759–16764. DOI: 10.1021/ja307061e
61. Para, F.; Bocquet, F.; Nony, L.; Loppacher, C.; Féron, M.; Cherioux, F.; Gao, D. Z.; Federici Canova, F.; Watkins, M. B. Micrometre-long covalent organic fibres by photoinitiated chain-growth radical polymerization on an alkali-halide surface. *Nature Chem.* **2018**, *10*, 1112–1117. DOI: 10.1038/s41557-018-0120-x